# Pseudo-rapidity distribution from a perturbative solution of viscous hydrodynamics for heavy ion collisions at RHIC and LHC *

Ze-Fang Jiang(江泽方)[1,2;1)] C. B. Yang(杨纯斌)[1,2;2)] Chi Ding(丁驰)[1,2] Xiang-Yu Wu(吴祥宇)[1,2]

[1] Key Laboratory of Quark and Lepton Physics, Ministry of Education, Wuhan, 430079, China
[2] Institute of Particle Physics, Central China Normal University, Wuhan 430079, China

**Abstract:** The charged-particle final state spectrum is derived from an analytic perturbative solution for relativistic viscous hydrodynamics. By taking into account the longitudinal acceleration effect in relativistic viscous hydrodynamics, the pseudorapidity spectrum describes the nucleus-nucleus colliding systems at RHIC and the LHC well. Based on both the extracted longitudinal acceleration parameter $\lambda^*$ and a phenomenological description of $\lambda^*$, the charged-particle pseudorapidity distributions for $\sqrt{s_{NN}}$ = 5.44 TeV Xe+Xe collisions are computed from the final state expression in a limited space-time rapidity $\eta_s$ region.

**Keywords:** viscous hydrodynamics, final state observable, pseudorapidity distributions, longitudinal acceleration effect, xenon+xenon collisions

**PACS:** 25.75.-q, 25.75.Nq **DOI:** 10.1088/1674-1137/42/12/123103

## 1 Introduction

Relativistic hydrodynamics seems to be an efficient tool to study the expansion and many non-equilibrium properties of quark-gluon plasma (QGP) produced in high energy heavy ion collisions, such as those at the Relativistic Heavy Ion Collider (RHIC) at Brookhaven National Laboratory, USA and the Large Hadron Collider (LHC) at CERN [1–3].

There has been tremendous theoretical [4–26] and numerical work [27–31] in solving relativistic hydrodynamic equations. These works not only simulate the fluid's dynamical evolution but also play an important role in extracting the transport properties of the strongly coupled matter. In our previous papers [32, 33], a series of exact solutions for a relativistic accelerating perfect fluid were presented and served as a reliable reference to study the longitudinal acceleration effect, pseudorapidity distributions and the initial state properties for colliding systems at RHIC and at the LHC [15, 17, 19, 32, 33].

In this paper, we expand the current knowledge of accelerating hydrodynamics [17, 32] by including the first-order viscous (Navier-Stokes limit) corrections in the relativistic domain. Based on a perturbative solution [34] which includes the longitudinal acceleration in relativistic viscous hydrodynamics, the final state observations which contain the longitudinal acceleration effect are derived. We find that the final state observations depend on the longitudinal acceleration parameter $\lambda^*$, and the pseudorapidity distribution can not only be used to compare the experimental data from the $\sqrt{s_{NN}}$ =130 GeV RHIC Au+Au collisions to the $\sqrt{s_{NN}}$ =5.02 TeV LHC Pb+Pb collisions [35–37], but also applied to study the longitudinal acceleration effect for nucleus-nucleus collisions at different $\sqrt{s_{NN}}$. Furthermore, motivated by the $^{129}$Xe+$^{129}$Xe run with $\sqrt{s_{NN}}$=5.44 TeV at the LHC in October 2017 and many other prospective Xe+Xe collision studies[38–40], the charged-particle pseudorapidity distribution for the most central Xe+Xe collisions with $\sqrt{s_{NN}}$=5.44 TeV is computed with this relativistic viscous hydrodynamics model and compared with the latest ALICE Collaboration data [41].

The organization of this paper is as follows. In Section 2, the transverse momentum spectrum and (pseudo-)rapidity spectrum are derived from a perturbative solution for relativistic viscous hydrodynamics. In Section 3, the pseudorapidity spectrum is used to study the longitudinal accelerating parameter $\lambda^*$ at RHIC and the LHC. A brief summary and discussion are given in Section 4.

## 2 Perturbative solution and final state observables

The basic formulation of relativistic hydrodynamics

Received 22 June 2018, Published online 19 October 2018

∗ Supported by National Natural Science Foundation of China (11435004), the Chinese-Hungarian bilateral cooperation program (Te'T 12CN-1-2012-0016) and the CCNU PhD Fund 2016YBZZ100 of China

1) E-mail: jiangzf@mails.ccnu.edu.cn

2) E-mail: cbyang@mail.ccnu.edu.cn

can be found in the literature [6, 19, 42]. In this paper, we consider a system with net conservative charge ($\mu_i = 0$). The flow velocity field is normalized to unity, $u^\mu u_\mu = 1$, and the metric tensor is chosen as $g_{\mu\nu}$=diag(1,−1,−1,−1).

The energy-momentum tensor $T^{\mu\nu}$ of the fluid system in the presence of viscosity is

$$T^{\mu\nu}=\varepsilon u^\mu u^\nu - P\Delta^{\mu\nu}+\Pi^{\mu\nu}, \tag{1}$$

where $\varepsilon$ and $P$ are the energy density and the local isotropic pressure, respectively. The equation of state (EoS) is $\varepsilon = \kappa P$. The viscous stress tensor is $\Pi^{\mu\nu} = \pi^{\mu\nu}-\Delta^{\mu\nu}\Pi$, where $\Pi$ is the bulk pressure, and $\pi^{\mu\nu}$ is the stress tensor [6]. $\Delta^{\mu\nu}=g^{\mu\nu}-u^\mu u^\nu$ and $\Delta^{\mu\nu}u_\nu=0$.

Following the conservation equations $\partial_\mu T^{\mu\nu}=0$, the energy equation and Euler equation are reduced to

$$D\varepsilon=-(\varepsilon+P+\Pi)\theta+\sigma_{\mu\nu}\pi^{\mu\nu}, \tag{2}$$

$$(\varepsilon+P+\Pi)Du^\alpha=\nabla^\alpha(P+\Pi)-\Delta^\alpha_\nu u_\mu D\pi^{\mu\nu}-\Delta^\alpha_\nu\nabla_\mu\pi^{\mu\nu}, \tag{3}$$

where shorthand notations for the differential operators $D=u^\mu\partial_\mu$, $\nabla^\alpha=\Delta^{\mu\alpha}\partial_\mu$ are introduced, with the expansion rate $\theta=\nabla_\mu u^\mu$. The shear tensor is

$$\sigma^{\mu\nu}\equiv\partial^{\langle\mu}u^{\nu\rangle}\equiv(\frac{1}{2}(\Delta^\mu_\alpha\Delta^\nu_\beta+\Delta^\mu_\beta\Delta^\nu_\alpha)-\frac{1}{d}\Delta^{\mu\nu}\Delta_{\alpha\beta})\partial^\alpha u^\beta. \tag{4}$$

Based on the Gibbs thermodynamic relation and the second law of thermodynamics, the simplest way to satisfy the constraint (entropy must always increase locally) is to impose the linear relationships between the thermodynamic forces and fluxes (in the Navier-Stokes limit [5, 6, 25, 42–45]),

$$\Pi=-\zeta\theta, \quad \pi^{\mu\nu}=2\eta\sigma^{\mu\nu}, \tag{5}$$

where the bulk viscosity $\zeta$ and the shear viscosity $\eta$ are two positive coefficients. Note that throughout this work we denote the shear viscosity as $\eta$, the space-time rapidity as $\eta_s$ and the particle pseudorapidity as $\eta_p$.

In the accelerating frame, the proper time $\tau=\sqrt{t^2-r^2}$ and space-time rapidity $\eta_s = \frac{1}{2}\log((t+r)/(t-r))$ are independent variables, where $r = \sqrt{\Sigma_i r_i^2}$ and $x^\mu = (t,r_1,\ldots,r_d)$ [17, 33]. The velocity field is parameterized as $v=\tanh(\Omega(\eta_s))$, with the flow-element rapidity $\Omega(\eta_s)$ being an arbitrary function of the coordinate $\eta_s$, and $\Omega$ is independent of the proper time $\tau$ [18]. (For simplicity, in the following we will use $\Omega$ to represent $\Omega(\eta_s)$, and $\Omega'$ stands for $\mathrm{d}\Omega/\mathrm{d}\eta_s$). With the special condition $\Omega(\eta_s)=\eta_s$, it can naturally come back to the Hwa-Bjorken case [14].

The energy equation Eq. (2) and the Euler equation Eq. (3) in Rindler coordinates reduce to the following two differential equations,

$$\tau\frac{\partial T}{\partial\tau}+\tanh(\Omega-\eta_s)\frac{\partial T}{\partial\eta_s}+\frac{\Omega'}{\kappa}T=\frac{\Pi_d}{\kappa}\frac{\Omega'^2}{\tau}\cosh(\Omega-\eta_s), \tag{6}$$

$$\begin{aligned}&\tanh(\Omega-\eta_s)\left[\tau\frac{\partial T}{\partial\tau}+T\Omega'\right]\\ =&\frac{\Pi_d}{\tau}(2\Omega'(\Omega'-1)-\frac{\partial T}{\partial\eta_s}+\Omega''\coth(\Omega-\eta_s))\sinh(\Omega-\eta_s),\end{aligned} \tag{7}$$

where $T$ is the temperature,

$$\varepsilon\propto T^{\kappa+1}, \qquad \Pi_d\equiv\left(\frac{\zeta}{s}+\frac{2\eta}{s}\left(1-\frac{1}{d}\right)\right)$$

is a combination of the shear viscosity and bulk viscosity, $s$ is the entropy density, and $d$ is the space dimension. $\eta/s$ and $\zeta/s$ are assumed to be constant in the following calculations [28, 46]. If $\Pi_d = 0$, the exact acceleration solutions of ideal hydrodynamic have already been presented in Refs. [17, 33].

We are interested in the viscous case ($\Pi_d \neq 0$) throughout this paper. One can see that it is difficult to find a general exact analytical solution for two partial differential equations Eqs. (6-7) for arbitrary $\Omega$. Fortunately, one can find a perturbative solution of these energy and Euler equations. Based on the results from the ideal hydro [32, 33], we assume the case in which $\Omega\equiv\lambda\eta_s\equiv(1+\lambda^*)\eta_s$, with $\lambda^*$ being the very small constant acceleration parameter ($0<\lambda^*\ll 1$). $\Omega'$ approximately characterizes the longitudinal acceleration of a flow element in the medium.

Up to the leading order $\mathcal{O}(\lambda^*)$, the combination of energy equation Eq. (6) and Euler equation Eq. (7) yields a partial differential equation depending only on $\tau$. The temperature solution $T(\tau,\eta_s)$ is

$$\begin{aligned}T(\tau,\eta_s)=&T_1(\eta_s)\left(\frac{\tau_0}{\tau}\right)^{\frac{1+\lambda^*}{\kappa}}\\ &+\frac{(2\lambda^*+1)\Pi_d}{(\kappa-1)\tau_0}\left(\frac{\tau_0}{\tau}\right)^{\frac{1+\lambda^*}{\kappa}}\left[1-\left(\frac{\tau_0}{\tau}\right)^{1-\frac{1+\lambda^*}{\kappa}}\right],\end{aligned} \tag{8}$$

where $\tau_0$ is the value of proper time, and $T_1(\eta_s)$ is an unfixed function.

Putting Eq. (8) into the Euler equation Eq. (7), up to $\mathcal{O}(\lambda^*)$, one gets

$$\begin{aligned}T_1(\eta_s)=&T_0\exp[-\frac{1}{2}\lambda^*(1-\frac{1}{\kappa})\eta_s^2]\\ &-\frac{\left(1-\exp[-\frac{1}{2}\lambda^*(1-\frac{1}{\kappa})\eta_s^2]\right)\Pi_d}{(\kappa-1)\tau_0},\end{aligned} \tag{9}$$

where $T_0$ defines the values for temperature at the proper time $\tau_0$ and coordinate rapidity $\eta_s$=0.

Finally, inputting Eq. (9) into Eq. (8), we obtain a perturbative analytical solution of the 1+1 D embed 1+3 D accelerating relativistic viscous hydrodynamics,

$$T(\tau,\eta_s)=T_0\left(\frac{\tau_0}{\tau}\right)^{\frac{1+\lambda^*}{\kappa}}\left[\exp\left(-\frac{1}{2}\lambda^*\left(1-\frac{1}{\kappa}\right)\eta_s^2\right)+\frac{R_0^{-1}}{\kappa-1}\left(2\lambda^*+\exp\left[-\frac{1}{2}\lambda^*\left(1-\frac{1}{\kappa}\right)\eta_s^2\right]-(2\lambda^*+1)\left(\frac{\tau_0}{\tau}\right)^{\frac{\kappa-\lambda^*-1}{\kappa}}\right)\right], \tag{10}$$

where the Reynolds number is $R_0^{-1}=\frac{\Pi_d}{T_0\tau_0}$ [6, 48].

The profile of $T(\tau,\eta_s)$ is a (1+1) dimensional scaling solution in (1+3) dimensions and it now contains not only acceleration but also viscosity dependent terms. The $\eta_s$ dependence is of the Gaussian form. Note that when $\lambda^*=0$ and $R_0^{-1}=0$, one obtains the same solutions as the ideal hydrodynamic [14]. When $\lambda^*=0$ and $R_0^{-1}\neq 0$, one obtains the first order Bjorken solutions [6, 43]. If $\lambda^*\neq 0$ and $R_0^{-1}=0$, one obtains a special solution which is consistent with case (c) of the CNC solutions in Refs. [17, 18]. Furthermore, this temperature profile (Eq. (10)) implies that for a non-vanishing acceleration $\lambda^*$, the cooling rate is larger than for the ideal case. Meanwhile, a non-zero viscosity makes the cooling rate smaller than for the ideal case [34].

The thermal spectrum of charged particles at proper time $\tau_f$ can be obtained from the Cooper-Frye flux term [49] and the temperature profile in Eq. (10),

$$\frac{\mathrm{d}^2N}{2\pi p_T\mathrm{d}p_T\mathrm{d}y}=\frac{g}{(2\pi)^3}\int p_\mu\mathrm{d}\Sigma^\mu f, \tag{11}$$

where $g$ is the spin-degeneracy factor, and $\Sigma$ is the freeze-out hypersurface.

For a system out of equilibrium, the particle phase-space distribution function $f$ contains not only the equilibrium distribution function $f_0$ but also the viscous corrections function $\delta f$. In a Boltzmann approximation, $f_0$ and $\delta f$ have been derived in Refs. [50, 51],

$$f_0=\exp\left(\frac{\mu_i(x)}{T}-\frac{p_\mu u^\mu}{T}\right), \tag{12}$$

$$\delta f=\frac{1}{2(\varepsilon+P)T^2}f_0p^\mu p^\nu\left[\pi_{\mu\nu}-\frac{2}{5}\Pi\Delta_{\mu\nu}\right], \tag{13}$$

where $\mu_i$ is the chemical potential and $T$ is the temperature. When net conservative charge is considered, $\mu_i=0$, and the particle momentum $p^\mu$ can be written as

$$p^\mu=(m_T\cosh y,p_T\cos\phi,p_T\sin\phi,m_T\sinh y), \tag{14}$$

with the transverse momentum $p_T$ and transverse mass $m_T=\sqrt{p_T^2+m^2}$, where $m$ is the charged particle mass, $y$ the particle rapidity, and $\phi$ the azimuthal angle. For an expanding Boltzmann gas, the thermal distribution is $f_0=\exp[-m_T\cosh(\Omega-y)/T]$. The freeze-out condition that the temperature at $\eta_s=0$ drops below a given $T_f$ value is assumed, with the four-velocity pseudo-orthogonal to the freeze-out hypersurface [17, 52, 53]. The freeze-out condition satisfies $\left(\frac{\tau_f}{\tau}\right)^{\Omega'-1}\cosh((\Omega'-1)\eta_s)=1$, and the integration measurement is

$$p_\mu\mathrm{d}\Sigma^\mu=m_T\tau_f\cosh^{\frac{2-\Omega'}{\Omega'-1}}((\Omega'-1)\eta_s)\cosh(\Omega-y)r\mathrm{d}r\mathrm{d}\phi\mathrm{d}\eta_s. \tag{15}$$

From the leading order condition, Eq. (10), the Cooper-Frye integration gives the thermal spectrum for the equilibrium state from an expanding cylinder geometry as

$$\frac{\mathrm{d}^2N^{(0)}}{2\pi p_T\mathrm{d}p_T\mathrm{d}y}=\frac{1}{(2\pi)^3}\int p_\mu\mathrm{d}\Sigma^\mu f_0=\frac{1}{(2\pi)^3}\int_0^{R_0}r\mathrm{d}r\int_0^{2\pi}\mathrm{d}\phi\int_{-\infty}^{+\infty}\mathrm{d}\eta_s m_T\tau_f\cosh^{\frac{1-\lambda^*}{\lambda^*}}(\lambda^*\eta_s)\cosh((\lambda^*+1)\eta_s-y)\times\exp\left[-\frac{m_T}{T(\tau,\eta_s)}\cosh((\lambda^*+1)\eta_s-y)\right]. \tag{16}$$

In the first order (Navier-Stokes) approximation and with the Gibbs relation $\varepsilon+P=Ts$, the first-order viscous correction to the spectrum is

$$\frac{\mathrm{d}^2N^{(1)}}{2\pi p_T\mathrm{d}p_T\mathrm{d}y}=\frac{\pi R_0^2}{(2\pi)^3}\int_{-\infty}^{+\infty}\mathrm{d}\eta_s\frac{(1+\lambda^*)m_T\cosh((\lambda^*+1)\eta_s-y)}{T^3(\tau,\eta_s)}\exp\left[-\frac{m_T}{T(\tau,\eta_s)}\cosh((\lambda^*+1)\eta_s-y)\right]\times\left[\frac{1}{3}\frac{\eta}{s}(p_T^2-2m_T^2\sinh^2((\lambda^*+1)\eta_s-y))+\frac{1}{5}\frac{\zeta}{s}(p_T^2+\sinh^2((\lambda^*+1)\eta_s-y))\right]. \tag{17}$$

Finally, an analytical expression of the transverse momentum distribution can be written as

$$\frac{\mathrm{d}^2N}{p_T\mathrm{d}p_T\mathrm{d}y}=\frac{\pi R_0^2}{(2\pi)^3}\int_{-\infty}^{+\infty}\mathrm{d}\eta_s m_T\cosh((\lambda^*+1)\eta_s-y)\exp\left[-\frac{m_T}{T(\tau,\eta_s)}\cosh((\lambda^*+1)\eta_s-y)\right]\times\left(\tau_f\cosh^{\frac{1-\lambda^*}{\lambda^*}}(\lambda^*\eta_s)+\frac{1+\lambda^*}{T^3(\tau,\eta_s)}\left[\frac{1}{3}\frac{\eta}{s}(p_T^2-2m_T^2\sinh^2((\lambda^*+1)\eta_s-y))\right.\right.$$

$$+\frac{1}{5}\frac{\zeta}{s}(p_T^2+m_T^2\sinh^2((\lambda^*+1)\eta_s-y))\Big]\Big), \tag{18}$$

where we can find that the transverse momentum distribution is sensitive to the viscosity.

One can make use of the condition $p_T\approx m_T$ (which is a good approximation for pions) and perform the integral of transverse momentum $p_T$. Then the rapidity distribution can be derived as

$$\frac{\mathrm{d}N}{\mathrm{d}y}=\frac{\pi R_0^2}{(2\pi)^3}\int_0^{+\infty}\mathrm{d}\eta_s\Big\{\cosh^{\frac{1-\lambda^*}{\lambda^*}}(\lambda^*\eta_s)\frac{4\tau_f T^3(\tau,\eta_s)}{\cosh^2((\lambda^*+1)\eta_s-y)}+\frac{48(1+\lambda^*)T^2(\tau,\eta_s)}{\cosh^4((\lambda^*+1)\eta_s-y)}$$
$$\times\Big[\frac{1}{3}\frac{\eta}{s}(1-2\sinh^2((\lambda^*+1)\eta_s-y))+\frac{1}{5}\frac{\zeta}{s}\cosh^2((\lambda^*+1)\eta_s-y)\Big]\Big\}. \tag{19}$$

Thus, the pseudorapidity distribution can be obtained from Eq. (18),

$$\frac{\mathrm{d}N}{\mathrm{d}\eta_p}=\frac{\pi R_0^2}{(2\pi)^3}\int_{-\infty}^{+\infty}\mathrm{d}\eta_s\int_0^{+\infty}\mathrm{d}p_T\sqrt{1-\frac{m^2}{m_T^2\cosh^2 y}}m_T p_T\cosh((\lambda^*+1)\eta_s-y)$$
$$\times\exp\Big[-\frac{m_T}{T(\tau,\eta_s)}\cosh((\lambda^*+1)\eta_s-y)\Big]\Big(\tau_f\cosh^{\frac{1-\lambda^*}{\lambda^*}}(\lambda^*\eta_s)+\frac{1+\lambda^*}{T^3(\tau,\eta_s)}$$
$$\times\Big[\frac{1}{3}\frac{\eta}{s}(p_T^2-2m_T^2\sinh^2((\lambda^*+1)\eta_s-y))+\frac{1}{5}\frac{\zeta}{s}(p_T^2+m_T^2\sinh^2((\lambda^*+1)\eta_s-y))\Big]\Big), \tag{20}$$

where $\eta_p$ is the pseudorapidity of the final hadron, and we have the relationship:

$$y=\frac{1}{2}\ln\frac{\sqrt{m^2+p_T^2\cosh^2\eta_p}+p_T\sinh\eta_p}{\sqrt{m^2+p_T^2\cosh^2\eta_p}-p_T\sinh\eta_p}.$$

## 3 Pseudorapidity distribution results

To go further and illustrate the effect of longitudinal acceleration on the observed final state spectra, a comparison between our hydrodynamic results and the RHIC and LHC data [35–37] is shown in this section.

In Fig. 1, the solid curves show the calculated pseudorapidity distribution. The normalization factor come from the most central multiplicity $\mathrm{d}N/\mathrm{d}\eta_p$ ($\eta_p=\eta_0$) with the parameters $\eta/s$=0.16 [28], $\zeta/s$=0.015 [46], and $T_f$=140 MeV. $\kappa=\frac{1}{c_s^2}=\frac{\partial\varepsilon}{\partial P}$ comes from the EoS table of the Wuppertal-Budapest lattice QCD calculation [54]. For simplicity, $\kappa$ is assumed to be a linear relationship for different colliding systems in this study. We use the relationship from the EoS table that $\kappa\approx7$ while $T\approx140$ MeV [30]. $m$=220±20 MeV is an approximate average mass of the final charged-particle ($\pi^{\pm}$, $K^{\pm}$, $p^{\pm}$) and it is calculated by a weighted average from the published experimental data [35, 36, 40, 47]. The freeze-out proper time is chosen as $\tau_f$=8 fm for nucleus-nucleus collisions. The rescatterings in the hadronic phase and the decays of hadronic resonances into stable hadrons are not included here. The acceptable integral region for each space-time rapidity is $-5.0\leq\eta_s\leq5.0$ (making sure the perturbative condition $\lambda^*\ll1$ is satisfied).

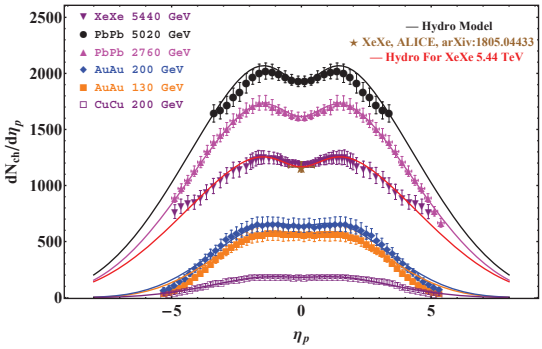


Fig. 1. (color online) Pseudorapidity distribution from our model calculation (solid curves) compared to the RHIC and LHC experiment data [35–37]. The red curve represents the pseudorapidity for Xe+Xe $\sqrt{s_{NN}}$ =5.44 TeV collisions. $\lambda^*_{\mathrm{Xe+Xe}}$= 0.030±0.003 comes from Eq.(21). Other parameters are consistent with Cu+Cu, Au+Au, and Pb+Pb. The computed centralmost multiplicity (five-pointed star) for Xe+Xe $\sqrt{s_{NN}}$ = 5.44 TeV is the normalization factor from the ALICE data [41], and the particle's multiplicity density prediction at forward rapidity and backward rapidity come from Eq. (20).

We then extracted the longitudinal acceleration parameter $\lambda^*$ for 130 GeV Au+Au, 200 GeV Au+Au, 200 GeV Cu+Cu, 2.76 TeV Pb+Pb, and 5.02 TeV Pb+Pb, the most central colliding systems without modifying any extra independent parameters. The extracted results for $\lambda^*$ are presented in Table 1. From this table, we obtain the same conclusion as in Ref. [33]: the higher centre-of-mass energy $\sqrt{s_{NN}}$ leads to both smaller longitudinal parameter $\lambda^*$ and higher multiplicity density at forward

and back pseudorapidity. However, because there is a different set-up of the number of free parameters in our paper and Ref. [33], the $\chi^2/NDF$ are different from the results in Ref. [33].

Table 1. Table of parameters from hydrodynamic fits in the text. Centrality for Au+Au and Cu+Cu is 0–6%, centrality for Pb+Pb and Xe+Xe is 0–5%. The $\chi^2$ is calculated from the statistical uncertainty.

| $\sqrt{s_{NN}}$/GeV | | $\frac{\mathrm{d}N}{\mathrm{d}\eta}\Big\vert_{\eta=\eta_0}$ | $\lambda^*$ | $\chi^2/NDF$ |
|---|---|---|---|---|
| 130 | Au+Au | 563.9±59.5 | 0.076±0.003 | 9.41/53 |
| 200 | Au+Au | 642.6±61.0 | 0.062±0.002 | 12.23/53 |
| 200 | Cu+Cu | 179.5±17.5 | 0.060±0.003 | 2.41/53 |
| 2760 | Pb+Pb | 1615±39.0 | 0.035±0.003 | 5.50/41 |
| 5020 | Pb+Pb | 1929±47.0 | 0.032±0.002 | 33.0/27 |
| 5440 | Xe+Xe | 1167±26.0[41] | 0.030±0.003 | −/− |

A phenomenological expression for $\sqrt{s_{NN}}$ and $\lambda^*$ is computed based on the $\lambda^*$ results in Table 1,

$$\lambda^*=A\left(\frac{\sqrt{s_{NN}}}{\sqrt{s_0}}\right)^{-B}, \tag{21}$$

where $\sqrt{s_0}=1$ GeV, $A=0.045$ and $B=0.23$ for nucleus-nucleus collisions[1)]. Based on Eq. (21), the longitudinal acceleration parameter $\lambda^*$ for the 0-5% centrality Xe+Xe $\sqrt{s_{NN}}=5.44$ TeV collisions are computed and we find $\lambda^*_{\mathrm{XeXe}}$=0.030±0.003. Using the same parameters as for the lower energy region and omitting other effects, the pseudorapidity distribution for Xe+Xe $\sqrt{s_{NN}}=5.44$ TeV collisions are computed and shown in Fig. 1. The red curve shows our model's calculations for the Xe+Xe colliding system. The hydrodynamics final state spectrum Eq. (20) can describe the experiment data well. On the basis of the predicted smaller longitudinal acceleration parameter $\lambda^*$ from Eq. (21), the Xe+Xe multiplicity gradient at $\sqrt{s_{NN}}=5.44$ TeV presents a smoother drop at forward and backward pseudorapidity than Cu+Cu collisions, Au+Au collisions and Pb+Pb collisions.

## 4 Discussion and conclusions

In conclusion, based on previous work [17, 32–34], a temperature profile is presented for accelerating relativistic viscous hydrodynamic equations by introducing a first-order correction to the conservation equations in Rindler coordinates. From such a temperature profile in 1+3-dimension space-time, the fluid evolution is generally decelerated due to the viscosity $\Pi^{\mu\nu}$. Meanwhile, the longitudinal accelerating effect of the flow-element compensates for the decrease of temperature gradient. These two opposite behaviors may provide a new perspective for studying the medium evolution thermodynamical quantities in viscous hydrodynamics. More detailed discussions are presented in Ref. [34].

Furthermore, based on the temperature profile and the Cooper-Frye flux term [49], three final state spectra, Eqs. (18, 19, 20), are obtained in this paper. We find the pesudorapidity distribution describes the experimental data well for the most central colliding systems at RHIC and the LHC. Also, as shown in Fig. 1, the smaller longitudinal acceleration parameter $\lambda^*$, the flatter the pseudorapidity distributions. In addition, the introduced longitudinal acceleration factor $\lambda^*$ has an interesting trend in that $\lambda^*$ is smaller for higher $\sqrt{s_{NN}}$. By using the measured longitudinal acceleration parameter $\lambda^*$ for different systems and assuming a phenomenological power function about $\lambda^*$, the pseudorapidity distribution for charged-particle in $\sqrt{s_{NN}}=5.44$ TeV Xe+Xe collisions are computed and describe the experimental data from the ALICE Collaboration [41] well.

In this study, we focused on derivations from final state observations and estimations of longitudinal acceleration effect. Many conditions applied in this model are still far from realistic heavy ion collisions. For a more realistic study based on or beyond this study, the following physical effects are important and should be taken into account. (a) The equation of state (EoS) at different temperatures should be close to the results from realistic lattice QCD calculations [54]. (b) The viscosity should depend on $\sqrt{s_{NN}}$ [28, 46]. (c) Statistical weights for the charged particle's mass should be calculated from experimental data [35, 36, 40, 47]. (d) The freeze-out hypersurface could be calculated by a smooth method [30] or other methods. (e) Resonance decays [55] and rescatterings in the hadronic phase [56] could be taken into account, and so on. Those important effects and conditions should be studied in our future research.

The final state spectra obtained in this paper may not only shed new light on the longitudinal acceleration effect of the medium's evolution, but could also serve as a test tool for hydrodynamic numerical codes [30] in the near future.

*We thank Xin-Nian Wang for a suggestion about xenon+xenon collisions. We thank Tamás Csörgő, Máté Csanád, Long-Gang Pang, T. S. Biró, Chao Wu for useful and inspiring discussions. We thank Wei Chen for a careful reading of this manuscript. Z-F. Jiang would like to thank Lévai Péter and Gergely Gábor Barnafoldi for kind hospitality during his stay at Winger RCP, Budapest, Hungary.*

1) This $A$ and $B$ should depend on $N_{\mathrm{part}}$, $N_{\mathrm{coll}}$ and other parameters. The problem will become clearer after comparing with more RHIC and LHC data in the near future.

## References


1 S. A. Bass, M. Gyulassy, H. Stöecker, and W. Greiner, J. Phys. G, **25**: R1-R57 (1999), arXiv: 9810281 [hep-ph]
2 M. Gyulassy and L. McLerran, Nucl. Phys. A, **750**: 30-63, arXiv: 0405013 [nucl-th]
3 U. Heinz and R. Snellings, Ann. Rev. Nucl. Part. Sci., **63**: 123-151 (2013), arXiv: 1301.2826 [nucl-th]
4 Paul. Romatschke and Ulrike. Romatschke, arXiv: 1712.05815 [nucl-th]
5 W. Israel and J. M. Stewart, Annals Phys., **118**: 341-372 (1979)
6 A. Muronga, Phys. Rev. C, **69**: 034904 (2004), arXiv: 0309055 [nucl-th]
7 R. Baier, P. Romatschke, D. T. Son, A. O. Starinets, and M. A. Stephanov, JHEP, **04**: 100 (2008), arXiv:0712.2451 [hep-th]
8 S. Bhattacharyya, V. E. Hubeny, S. Minwalla, and M. Rangamani, JHEP, **02**: 045 (2008), arXiv: 0712.2456 [hep-th]
9 T. Koide, G. S. Denicol, P. Mota, and T. Kodama, Phys. Rev. C, **75**: 034909 (2007), arXiv: 0609117 [hep-ph]
10 J. Peralta-Ramos and E. Calzetta, Phys. Rev. D, **80**: 126002 (2009), arXiv: 0908.2646 [hep-ph]
11 G. S. Denicol, H. Niemi, E. Molnár, and D. H. Rischke, Phys. Rev. D, **85**: 114047 (2012), arXiv: 1202.4551 [nucl-th]
12 L. D. Landau, Izv. Akad. Nauk Ser. Fiz., **17**: 51 (1953)
13 R. C. Hwa, Phys. Rev. D, **10**: 2260 (1974)
14 J. D. Bjorken, Phys. Rev. D, **27**: 140 (1983)
15 T. S. Biró, Phys. Lett. B, **487**: 133 (2000), arXiv: 0003027 [nucl-th]
16 T. Csörgő, F. Grassi, Y. Hama, and T. Kodama, Phys. Lett. B, **565**: 107 (2003), arXiv: 0305059 [nucl-th]
17 T. Csörgő, M. I. Nagy, and M. Csanád, Phys. Lett. B, **663**: 306 (2008), arXiv: 0605070 [nucl-th]
18 M. I. Nagy, T. Csörgő, and M. Csanád, Phys. Rev. C, **77**: 024908 (2008)
19 M. I. Nagy, Phys. Rev. C, **83**: 054901 (2011), arXiv: 0909.4286 [nucl-th]
20 S. S. Gubser, Phys. Rev. D, **82**: 085027 (2010), arXiv: 1006.0006 [hep-th]
21 S. S. Gubser and A. Yarom, Nucl. Phys. B, **846**: 469 (2011), arXiv: 1012.1314 [hep-th]
22 Z. J. Jiang, K. Ma, H. L Zhang, and L. M. Cai, Chin. Phys. C, **38**: 084103 (2014)
23 Z. J. Jiang, J. Wang, H. L. Zhang, and K. Ma, Chin. Phys. C, **39**: 044102 (2015)
24 Y. Hatta, J. Noronha, and Bo-Wen Xiao, Phys. Rev. D, **89**: 051702 (2014), arXiv: 1401.6248 [nucl-th]
25 Y. Hatta, J. Noronha, and Bo-Wen Xiao, Phys. Rev. D, **89**: 114011 (2014), arXiv: 1403.7693 [nucl-th]
26 Chao Wu, Yidian Chen, and Mei Huang, JHEP, **03**: 082 (2017) arXiv: 1608.04922 [hep-th]
27 Schenke, Bjorn, Jeon, Sangyong, and Gale, Charles, Phys. Rev. Lett., **106**: 042301 (2011) arXiv: 1009.3244 [hep-ph]
28 Song Huichao, Bass Steffen A., Heinz Ulrich, Hirano Tetsufumi, and Shen Chun, Phys. Rev. Lett., **106**: 192301, arXiv: 1011.2783 [nucl-th]
29 K .Werner, Iu. Karpenko, T. Pierog, M. Bleicher, and K. Mikhailov, Phys. Rev. C, **82**: 044904 (2010), arXiv: 1004.0805 [nucl-th]
30 Long-Gang Pang, Petersen Hannah, and Xin-Nian Wang, arXiv: 1802.04449 [nucl-th]
31 Wei Chen, Shanshan Cao, Tan Luo, Long-Gang Pang, and Xin-Nian Wang, Phys. Let. B, **777**: 86 (2018), arXiv: 1704.03648 [nucl-th]
32 M. Csanád, T. Csörgő, Ze-Fang. Jiang, and C. B. Yang, Universe. 3, **1**: 9 (2017), arXiv: 1609.07176
33 Ze-Fang. Jiang, C. B. Yang, M. Csanád, and T. Csörgő, Phys. Rev. C, **97**: 064906 (2018), arXiv: 1711. 10740
34 Ze-Fang Jiang, C. B. Yang, M. Csanád, T. Csörgő, G. Kasza, and M. I. Nagy in preparing
35 B. Alver et al (PHOBOS Collaboration), Phys. Rev. C, **83**: 024913(2011), arXiv: 1011.1940 [nucl-th]
36 J. Adam and et al (ALICE Collaboration), Phys. Lett. B, **754**: 373 (2016), arXiv: 1509.07299 [nucl-ex]
37 J. Adam and et al (ALICE Collaboration), Phys. Lett. B, **772**: 567, arXiv: 1612.08966 [nucl-ex]
38 Giacalone Giuliano, Noronha-Hostler Jacquelyn, Luzum Matthew, and Ollitrault Jean-Yves, Phys. Rev. C, **97**: 034904 (2018), arXiv: 1711.08499 [nucl-th]
39 K. J. Eskola, H. Niemi, R. Paatelainen, and K. Tuominen, Phys. Rev. C, **97**: 034911 (2018), arXiv: 1711.09803 [hep-ph]
40 Leonard S. Kisslinger and Debasish Das, arXiv: 1801.03826 [hep-ph]
41 Acharya, Shreyasi, and others (ALICE collaboration) arXiv: 1805.04432 [nucl-ex]
42 P. Romatschke, Int. J. Mod. Phys. E, **19**: 1-53 (2010), arXiv: 0902.3663v3 [hep-ph]
43 D.Teaney, Phys. Rev. C, **68**: 034913 (2003), arXiv: 0301099 [nucl-th]; 0209024 [nucl-th]
44 M. Damodaran, D. Molnár, G. G. Barnaföldi, D. Berényi, and M. F. Nagy-Egri, arXiv: 1707.00793 [nucl-th]
45 S. Weinberg, *Gravitation and cosmology: Princles and Applications of the General Theory of Relativity*, (Wiley, New York, 1972)
46 H. B. Meyer, Phys. Rev. Lett., **100**: 162001 (2008), arXiv: 0710.3717 [hep-lat]
47 A. Adare and others (PHENIX Collaboration), Phys. Rev. Lett., **95**: 162301 (2007) arXiv: 0608033 [nucl-ex]
48 H. Kouno, M. Maruyama, F. Takagi, and K. Saito, Phys. Rev. D, **41**: 2903 (1990)
49 F. Cooper and G. Frye, Phys. Rev. D, **10**: 186 (1974)
50 K. Dusling and D. Teaney, Phys. Rev. C, **77**: 034905 (2008), arXiv:0710.5932 [nucl-th]
51 K. Dusling, G. D. Moore, and D. Teaney, Phys. Rev. C, **81**: 034907 (2010), arXiv: 0909.0754 [nucl-th]
52 M. Csanád and T. Csörgő, J. Phys. G, **30**: S1079-S1082 (2004), arXiv: 0403074 [nucl-th]
53 M. Csanád, T. Csörgő, B. Lörstad, and A. Ster, AIP Conf. Proc., **828**: 479 (2005), arXiv: 0510027 [nucl-th]
54 P. Huovinen and P. Petreczky, Nucl. Phys. A, **837**: 26 (2010), arXiv: 0912.2541[hep-ph]
55 P. Alba et al, Phys. Rev. D, **96**(3): 034517 (2017), doi: 10.1103/PhysRevD.96.034517, arXiv: 1702.01113 [hep-lat]
56 H. Song, S. A. Bass, U. Heinz, T. Hirano, and C. Shen, Phys. Rev. C, **83**: 054910 (2011) Erratum: [Phys. Rev. C, **86**: 059903 (2012)], doi: 10.1103/PhysRevC.83.054910, 10.1103/PhysRevC.86.059903, arXiv: 1101.4638 [nucl-th]